Scripta Materialia 155 (2018) 73–77

Contents lists available at ScienceDirect

Scripta Materialia

journal homepage: www.elsevier.com/locate/scriptamat

Regular Article

Nano-laminated thin film metallic glass design for outstanding mechanical properties

P. Kontis [a,*], M. Köhler [a], S. Evertz [b], Y.-T. Chen [b], V. Schnabel [b], R. Soler [a], J. Bednarick [c], C. Kirchlechner [a], G. Dehm [a], D. Raabe [a], J.M. Schneider [b], B. Gault [a]

[a] Max-Planck-Institut für Eisenforschung, Max-Planck-Str. 1, 40237 Düsseldorf, Germany.
[b] Materials Chemistry, RWTH Aachen University, Kopernikusstr. 10, D-52074 Aachen, Germany
[c] Deutsches Elektronen Synchrotron DESY, FS-PE group, Notkestrasse 85, D-22607 Hamburg, Germany

ARTICLE INFO

Article history:
Received 9 April 2018
Received in revised form 6 June 2018
Accepted 6 June 2018
Available online xxxx

Keywords:
Thin film metallic glasses
Hybridization
Fracture toughness
Atom probe tomography

ABSTRACT

We report the enhancement of fracture toughness and strength of a cobalt tantalum-based metallic glass thin film with increasing boron content. The improvement of the mechanical performance is attributed to the formation of a compositionally lamellar compared to uniform glass microstructure, which becomes thinner with increasing boron content as revealed by transmission electron microscopy. Compositional variations across the lamellar structure are revealed by atom probe tomography. Cobalt- and boron-rich regions alternate sequentially, whereas tantalum exhibits slight variations across the lamellae. Our results can be utilized in future design efforts for metallic glass thin films with outstanding mechanical performance.

Metallic glasses exhibit a combination of high strength and toughness which make them an interesting material class for applications such as micro-gears, for instance in high precision endoscopes [1, 2]. However, as these medical tools continuously decrease in size, micro-gears need to decrease in size accordingly, resulting in increased applied stresses during operation. In order to reduce the risk of brittle failure, tougher metallic glasses with high strength are required in that context [3].

For the design of tough metallic glasses, a universal relationship between Poisson's ratio and brittle-ductile transition has been suggested by Lewandowski et al. in 2005 [4]. However, as only the elastic behavior of metallic glasses is considered by the Poisson's ratio, there is an ongoing discussion in literature about the reliability of this criterion regarding ductility [5–8]. Based on theoretical and experimental data of Co—Cu and Pd-based metallic glass systems, we have recently demonstrated that Poisson's ratio alone is not a universal predictor of the brittle-ductile transition. Instead we have proposed a design concept for damage-tolerant metallic glasses, where the low fraction of bonds stemming from hybridized states compared to the overall bonding serves as a fingerprint for damage tolerance [9]. While this assessment is based on a theoretical and experimental appraisal of homogeneous metallic glass systems which are without exception consistent with the notion put forward in Schnabel et al. [9], the here reported nano-lamellar Co-based metallic glass exhibiting a record fracture strength cannot be predicted based on any design notion available today.

To evaluate the influence of metal-metalloid bonding on the stiffness and damage-tolerance of metallic glasses, we have systematically investigated the influence of Co—B bonds in combinatorial Co-Ta-B metallic glass thin films (MGTFs) by experimental and theoretical methods. In this study, Co-Ta-B MGTFs were magnetron sputtered on Si (100) wafers with a diameter of 50.8 mm for chemical and mechanical characterization as well as on polyimide substrates for synchrotron X-ray diffraction (XRD) for topology analysis [10]. Data from 2D-XRD analysis of a representative film and with a substrate is shown in Supplementary Fig. 1. A lab-scale ultrahigh vacuum chamber was utilized for the production of the MGTFs and it was operated at a base pressure in the range of $5{\cdot}10^{-6}$ Pa. A $Co_{88}Ta_{12}$ and a B target were used for the deposition with a purity of 99.9% and 99.5%, respectively. The magnetrons were tilted 45° from the substrate normal and no substrate rotation was employed. For the CoTa compound and B elemental targets, a direct current and radio frequency power supply were used, respectively. The power densities applied were 0.4 W/cm^2 for the CoTa target and 8.4 W/cm^2 for the B target. A film thickness of 2.5 μm was obtained.

Micro-cantilever bending experiments were carried out in situ in a scanning electron microscope (JEOL-JSM 2000) equipped with an ASMEC UNAT-2 indenter. 80 cantilevers were micro-machined using a focused ion-beam (FIB) microscope (FEI Helios NanoLab 600i dual-beam FIB) following the procedure described in Ref. [11]. A schematic illustration of the lamellae orientation with respect to nanoindentation and cantilever tests is shown in the Supplementary Fig. 2. Prior to FIB

* Corresponding author.
E-mail address: p.kontis@mpie.de (P. Kontis).

https://doi.org/10.1016/j.scriptamat.2018.06.015
1359-6462/

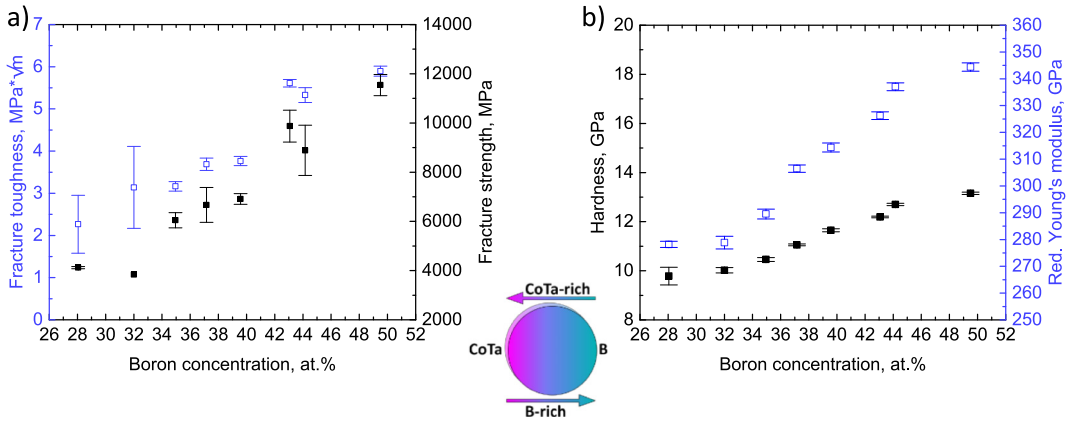

Fig. 1. Micro-mechanical testing of the combinatorial CoTaB metallic glass thin film. a) Fracture toughness and fracture strength graphs as a function of boron content as revealed by micro-cantilever bending tests. b) Young's modulus and hardness as a function of boron content measured by nanoindentation. The error bars correspond to the standard deviation.

milling, a free-standing film was obtained by selectively etching away the Si substrate, using a 30% KOH solution at 80 °C for 45 min [12, 13]. Five un-notched and five pre-notched cantilevers with size 18 × 2.5 × 2.5 μm^3 were fabricated and tested for eight different compositions to measure fracture strength and fracture toughness.

Bending tests were carried out in displacement-controlled mode using a constant displacement rate of 5 nm/s. A conical tip (1 μm tip radius) was employed for the experiments. Fracture toughness, K_{IC}, was evaluated following linear elastic fracture mechanics (LEFM):

$$K_{IC} = \frac{F_{max}\, L}{B\, w^{\frac{3}{2}}}\, f\left(\frac{a}{w}\right) \tag{1}$$

where F_{max} is the maximum load before fracture, L is the beam length, B the beam width, w the beam thickness, and a the notch depth of the pre-notch cantilevers. The function $f(a/w)$ is a shape factor and was determined by Matoy et al. [14] using FEM simulations. Cantilevers without pre-notch were used to calculate the fracture strength, σ_f, evaluated following classical bending beam theory:

$$\sigma = 6\,\frac{F_{max}\, l}{B\, w2} \tag{2}$$

For the structural and chemical characterization of the MGTFs transmission electron microscopy (TEM) and atom probe tomography (APT) were utilized. Samples for TEM investigation were fabricated with an FEI Helios NanoLab 600 followed by a post thinning-process with illumination of 500 eV ion beam. Micrographs were recorded in an FEI Titan G2 80–200 CREWLEY at 200 kV with a high angle annular dark field (HAADF) detector with camera length of 110 mm, and a device controlling system of DigiScan and Digital Micrograph. Site-specific 3D-APT samples were prepared using an FEI Helios NanoLab 600i dual-beam FIB. The APT specimens were prepared following the standard lift-out process [15]. The APT measurements were performed on a commercial CAMECA local electrode atom probe LEAP 3000X HR, in voltage mode at a base temperature of 60 K, pulse repetition rate of 200 kHz and pulse fraction of 15%.

Topological analysis was performed by synchrotron X-ray diffraction at beamline P02.1 at the electron storage ring PETRA III (DESY, Hamburg, Germany). The X-ray diffraction was carried out in transmission along the CoTa-B compositional gradient of the MGTFs deposited on polyimide foil [16]. A monochromatic photon beam with a spot size of 0.7 mm × 0.7 mm and a wavelength of 0.02070 nm was used. The diffracted 2D patterns were recorded with a fast image plate detector Perkin Elmer 1621, positioned at a distance of 238 mm from the thin film. The sample to detector distance, orthogonality of the detector and beam centre was calibrated using a CeO_2 powder standard (National Institute of Standards and Technology 674b). Individual diffraction patterns were acquired for 30 s. The diffraction patterns were integrated into q-space ($q = 4\pi \sin\theta/\lambda$) up to 18 Å^{-1} using the FIT2D software package [17]. The pair distribution functions (PDF) were obtained from the integrated diffraction intensity after correction for background contributions, sample absorption, inelastic scattering and normalization to the atomic X-ray form factor employing the PDFgetX2 software [18].

Finally, *ab initio* molecular dynamic simulations with the density functional theory [19] based openMX code [20, 21] were carried out. Electronic potentials with the generalised gradient approximation were employed [22]. Basis functions were linear combinations of localised pseudoatomic orbitals [23]. The following basis functions were applied: Co5.5-s2p1d1, Ta7.0-s2p1d1f1, B4.5-s2p2. The first symbol designates the chemical element followed by the cutoff radius. The last set of symbols defines the primitive orbitals. An N-point grid of 85 × 85 × 85 and a cutoff energy of 150 Ry has been used. For volume relaxation at 0 K the Vienna Ab-initio Simulation Package was utilized [24, 25]. Thereby, the ultrasoft pseudopotentials were employed and the Brillouin zone was integrated on a 3 × 3 × 3 Monkhorst-Pack k-point grid [26]. To model the short range ordered structure of the metallic glass, the structural model introduced by Hostert et al. [27] was applied with a supercell containing 115 atoms and 13 vacancies. In order to obtain an amorphous structure, the supercell was heated to 4000 K

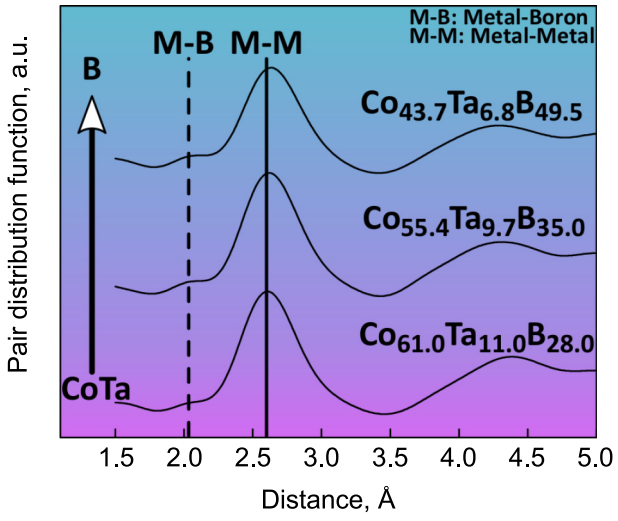

Fig. 2. Pair distribution functions with increasing B-content from bottom to top as obtained by high energy X-ray diffraction are presented in a range between 1.5 and 5.0 Å.